CONFIRMATION OF C_{60} IN THE REFLECTION NEBULA NGC 7023

K. Sellgren[1], M.W. Werner[2], J.G. Ingalls[3], J.D.T. Smith[4], T.M. Carleton[5] and C. Joblin[6, 7]

Abstract. The fullerene C_{60} has four infrared active vibrational transitions at 7.0, 8.5, 17.5 and 18.9 μm. We have previously observed emission features at 17.4 and 18.9 μm in the reflection nebula NGC 7023 and demonstrated spatial correlations suggestive of a common origin. We now confirm the identification of these features with C_{60} by detecting a third emission feature at 7.04 ± 0.05 μm at a position of strong 18.9 μm emission in NGC 7023. We also report the detection of these three features in the reflection nebula NGC 2023. We show with spectroscopic mapping of NGC 7023 that the 18.9 μm feature peaks on the central star, that the 16.4 μm emission feature due to PAHs peaks between the star and a nearby photodissociation front, and that the 17.4 μm feature is a blend of a PAH feature and C_{60}. The derived C_{60} abundance is consistent with that from previous upper limits and possible fullerene detections in the interstellar medium.

1 Introduction

Fullerenes are cage-like molecules (spheroidal or ellipsoidal) of pure carbon, such as C_{60}, C_{70}, C_{76}, and C_{84}. C_{60} is the most stable fullerene and can account for up to 50% of the mass of fullerenes generated in the laboratory (Kroto *et al.* 1985). Foing & Ehrenfreund (1994) propose that two diffuse interstellar bands at 958 and 963 nm are due to singly ionized C_{60}, or C_{60}^{+}, although the identification is debated

---

[1] Department of Astronomy, Ohio State University

[2] Jet Propulsion Laboratory, California Institute of Technology

[3] Spitzer Science Center, California Institute of Technology

[4] Ritter Astrophysical Research Center, University of Toledo

[5] University of Arizona

[6] Université de Toulouse, UPS, CESR

[7] CNRS

(Maier 1994; Jenniskens *et al.* 1997). Misawa *et al.* (2009) attribute additional diffuse interstellar bands at 902, 921, and 926 nm to C_{60}^+. Observational evidence for neutral fullerenes, however, has been elusive to date. No fullerenes have yet been found towards carbon-rich post-AGB stars (Somerville & Bellis 1989; Snow & Seab 1989), carbon stars (Clayton *et al.* 1995; Nuccitelli *et al.* 2005), or R CrB stars (Clayton *et al.* 1995; Lambert *et al.* 2001). Similarly, no neutral fullerenes have yet been found in the diffuse interstellar medium (Snow & Seab 1989; Herbig 2000), dense molecular clouds (Nuccitelli *et al.* 2005), or at the photodissociation front in the reflection nebula NGC 7023 (Moutou *et al.* 1999).

C_{60} has four infrared-active vibrational transitions, at 7.0, 8.5, 17.4, and 18.9 μm (Frum *et al.* 1991; Sogoshi *et al.* 2000). We tentatively identified the 17.4 and 18.9 μm interstellar emission features in the reflection nebula NGC 7023 as due to C_{60} (Werner *et al.* 2004b; Sellgren *et al.* 2007).

We report here the detection of the C_{60} feature at 7.04 $\pm$ 0.05 μm in NGC 7023. We also report the detection of C_{60} features at 7.04, 17.4 and 18.9 μm in a second reflection nebula, NGC 2023. The C_{60} 8.5 μm feature is too blended with the strong 8.6 μm PAH feature to yield a useful limit. We have found earlier (Sellgren *et al.* 2007) that the 18.9 μm emission feature in NGC 7023 has a spatial distribution distinct from that of the 16.4 μm emission feature attributed to polycyclic aromatic hydrocarbons (PAHs). We now compare the spatial distributions of the 16.4, 17.4, and 18.9 μm emission features in NGC 7023, and find additional suppport for the C_{60} identification.

2 Results

We have used the *Spitzer Space Telescope* (Werner *et al.* 2004a) with the Infrared Spectrograph (IRS; Houck *et al.* 2004) to obtain spectra of NGC 7023 and NGC 2023. We used the short-wavelength low-resolution module SL (5–14 μm; $\Delta\lambda/\lambda = 60$–120) and the long-wavelength low-resolution module LL2 (14–20 μm; $\Delta\lambda/\lambda = 60$–120). Nebular positions were chosen for a strong ratio of the 18.9 μm feature relative to the 16.4 μm PAH feature. We also made a spectroscopic map with the LL2 module of NGC 7023.

We show our 14–20 μm spectrum of NGC 2023 in Figure 1. We mark the wavelengths of C_{60} lines at 17.4 and 18.9 μm, of a PAH feature at 16.4 μm, and of H_2 emission at 17.0 μm.

We show our 5–9 μm spectra of NGC 7023 in Figure 2. We clearly detect an emission feature at 7.04 $\pm$ 0.05 μm. We detect the 7.04 μm feature also in NGC 2023. This feature is coincident, within the uncertainties, with the wavelength of the expected C_{60} line. We highlight this emission feature by fitting the 5–9 μm spectrum with a blend of PAH emission features in addition to the new emission feature at 7.04 μm. We perform this model fit using PAHFIT (Smith *et al.* 2007a).

In our previous long-slit spectroscopic investigation of NGC 7023 (Sellgren *et al.* 2007), we found that the 18.9 μm feature peaks closer to the central star than either neutral PAHs or ionized PAHs. We now use the LL2 spectroscopic
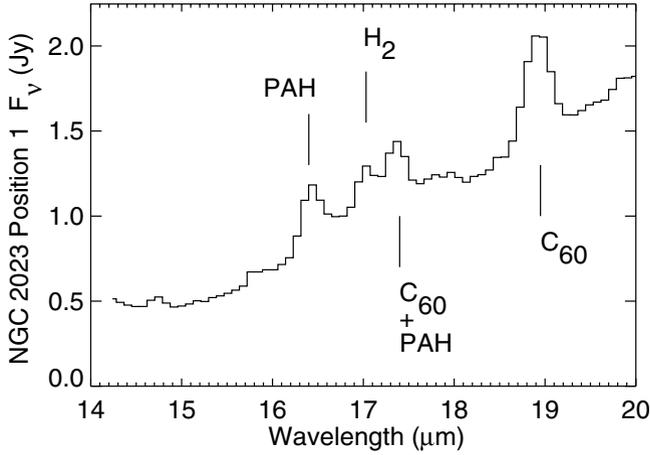
Fig. 1. *Spitzer*-IRS spectrum of NGC 2023 *(solid black histogram)*, obtained with the long-wavelength low-resolution module (LL2; 14–20 μm; $\lambda/\Delta\lambda = 60$–130). We mark the wavelengths of C$_{60}$ at 17.4 and 18.9 μm, a PAH feature at 16.4 μm, and H$_2$ emission at 17.0 μm *(vertical solid lines)*.

map extracted in NGC 7023 to illustrate this point more clearly in Figure 3. The 18.9 μm emission is clearly centered on the star. By contrast, the 16.4 μm PAH emission peaks outside the region of maximum 18.9 μm emission, in a layer between the star and the molecular cloud. The photodissociation front at the UV-illuminated front surface of the molecular cloud is delineated by fluorescent H$_2$ emission at 17.0 μm.

We show an image of the 17.4 μm emission from NGC 7023 in Figure 3, overlaid with contours of 18.9 μm and 16.4 μm emission. The 17.4 μm emission clearly shows one peak on the central star, coincident with the 18.9 μm C$_{60}$ emission, and a second peak co-spatial with the 16.4 μm PAH emission. We conclude that the observed 17.4 μm emission feature is a blend of a PAH feature at 17.4 μm, whose spatial distribution follows that of the 16.4 μm PAH feature, and of 17.4 μm C$_{60}$ emission.

3   Discussion

We have detected three lines due to C$_{60}$, in two reflection nebulae. This is the first detection of neutral C$_{60}$ in space.

Theorists have suggested that fullerenes might form around stars with carbon-rich atmospheres, such as carbon stars, cool carbon-rich Wolf-Rayet (WC) stars, and C-rich, H-poor R Cr B stars (Kroto & Jura 1992; Goeres & Sedlmayr 1992; Cherchneff *et al.* 2000; Pascoli & Polleux 2000). Fullerenes may also form as
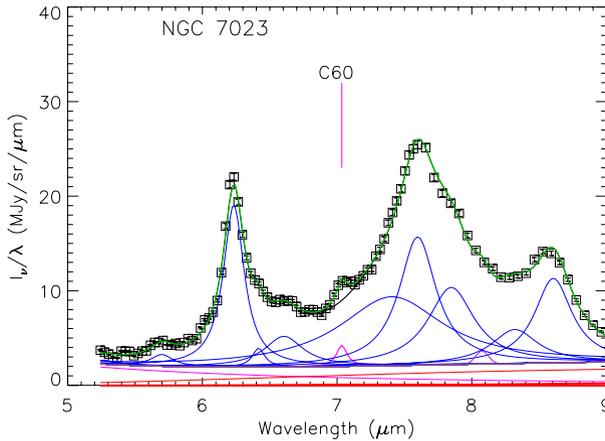
Fig. 2. *Spitzer*-IRS 5–9 μm spectrum of NGC 7023, obtained with the short-wavelength low-resolution module (SL; $\lambda/\Delta\lambda = 60$–120; solid black histogram). The wavelength of C_{60} at 7.0 μm is marked (vertical solid magenta line). We show the individual contributions of PAH features at 5.3, 5.7, 6.2, 6.4, 6.7, 7.4, 7.6, 7.8, 8.3, and 8.6 μm to the spectrum, by decomposing the spectrum with PAHFIT (Smith *et al.* 2007a) and then overplotting the Lorentzian profile of each feature (thin solid black curves). The Lorentzian fit to the C_{60} feature we detect at 7.04 $\pm$ 0.05 μm is highlighted (thick solid magenta curve).

part of the carbon-rich grain condensation process known to occur in the ejecta of Type II supernovae (Clayton *et al.* 2001). Fullerenes might form via interstellar gas-phase chemistry in dense and diffuse molecular clouds (Bettens & Herbst 1996, 1997). Hydrogenated amorphous carbon grains in the interstellar medium may also decompose after interstellar shocks into fullerenes and PAHs (Scott *et al.* 1997).

We compare the relative amounts of stellar flux absorbed and re-radiated by fullerenes and PAHs to derive the abundance of C_{60} in NGC 7023 and NGC 2023. First we compare the sum of the intensities of the 7.0, 17.4, and 18.9 μm features, assumed to be due to C_{60}, to the sum of all other infrared emission features at 5–20 μm, assumed to be due to PAHs. We ignore potential visual fluorescence by C_{60} or PAHs, do not include any potential 8.5 μm C_{60} emission, and do not attempt to correct the 17.4 μm C_{60} emission for any PAH contribution. We used PAHFIT (Smith *et al.* 2007a) to find that the ratio of C_{60} to PAH emission is 0.01–0.03 in NGC 7023 and NGC 2023. We then compare the amount of UV starlight per C atom absorbed by C_{60} (Yasumatsu *et al.* 1996; Yagi *et al.* 2009). and PAHs (Li & Draine 2001). We assume that 9–18% of interstellar carbon is in PAHs (Joblin *et al.* 1992; Tielens 2008). Our preliminary estimate of the percentage of interstellar carbon contained in C_{60}, $p(C_{60})$, is 0.1–0.6%.
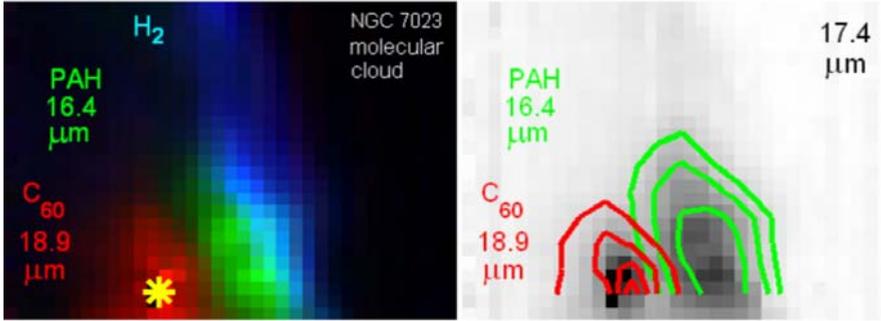
Fig. 3. Spectral map of NGC 7023, obtained with the *Spitzer* IRS 15–20 μm LL2 long-slit module, extracted and analyzed using CUBISM (Smith *et al.* 2007b). Each pixel is $5.1'' \times 5.1''$. *Left:* three-color image of NGC 7023, with the 18.9 μm C$_{60}$ feature in red, the 16.4 μm PAH feature in green, and the 17.0 μm H$_2$ line in blue. The position of the central star is marked with a cross. The 18.9 μm C$_{60}$ feature peaks on the central star. The front surface of the UV-illuminated molecular cloud is traced by H$_2$ emission, while the 16.4 μm PAH emission peaks between the C$_{60}$ and H$_2$ emission. *Right:* gray-scale image of NGC 7023 in the 17.4 μm feature, overlaid with contours of 18.9 μm C$_{60}$ emission *(red)*, and contours of 16.4 μm PAH feature emission *(green)*. The observed 17.4 μm emission has two spatial components, one co-spatial with C$_{60}$ emission and the other co-spatial with PAH emission. We conclude that the 17.4 μm emission feature is due to a blend of PAH and C$_{60}$ emission.

Our preliminary estimate of $p(C_{60})$ is consistent with published estimates of the percentage of carbon in C$_{60}^{+}$ in diffuse clouds (0.1–0.9%; Foing & Ehrenfreund 1994; Herbig 2000). It is also consistent with previous upper limits on $p(C_{60})$ towards R Coronae Borealis, massive young stellar objects, and NGC 7023 (<0.3–0.6%; Moutou *et al.* 1999; Nuccitelli *et al.* 2005).

4   Conclusions

We confirm our previous suggestion that emission features at 17.4 and 18.9 μm in NGC 7023 are due to C$_{60}$, by detecting a third C$_{60}$ line at 7.04 μm. We detect the 7.04, 17.4, and 18.9 μm C$_{60}$ lines in NGC 2023 also. The spatial distribution of the 17.4 μm feature in NGC 7023, compared to the spatial distributions of 16.4 μm PAH and 18.9 μm C$_{60}$ emission, suggests that the observed 17.4 μm feature is a superposition of two lines, one due to PAHs and one due to C$_{60}$. The abundance we derive for C$_{60}$ is consistent with previous upper limits on C$_{60}$ and previous measurements of lines identified with C$_{60}^{+}$. Our observations are the first firm detection of C$_{60}$ in space.

This work is based on observations made with the Spitzer Space Telescope, which is operated by the Jet Propulsion Laboratory, California Institute of

References

Bettens, R.P.A., & Herbst, E., 1997, ApJ, 478, 585

Bettens, R.P.A., & Herbst, E., 1996, ApJ, 468, 686

Cherchneff, I., Le Teuff, Y.H., Williams, P.M., & Tielens, A.G.G.M., 2000, A&A, 357, 572

Clayton, D.D., Deneault, E.A.-N., & Meyer, B.S., 2001, ApJ, 562, 480

Clayton, G.C., Kelly, D.M., Lacy, J.H., *et al.*, 1995, AJ, 109, 2096

Foing, B.H., & Ehrenfreund, P., 1994, Nature, 369, 296

Frum, C.I., Engleman, R.J., Hedderich, H.G., *et al.*, 1991, Chem. Phys. Lett., 176, 504

Goeres, A., & Sedlmayr, E., 1992, A&A, 265, 216

Herbig, G.H., 2000, ApJ, 542, 334

Houck, *et al.*, 2004, ApJS, 154, 18

Jenniskens, P., Mulas, G., Porceddu, I., & Benvenuti, P., 1997, A&A, 327, 337

Kroto, H.W., Heath, J.R., O'Brien, S.C., Curl, R.F., & Smalley, R.E., 1985, Nature, 318, 162

Joblin, C., Léger, A., & Martin, P., 1992, ApJ, 393, L79

Kroto, H.W., & Jura, M., 1992, A&A, 263, 275

Lambert, D.L., Rao, N.K., Pandey, G., & Ivans, I.I., 2001, ApJ, 555, 925

Li, A., & Draine, B.T., 2001, ApJ, 554, 778

Maier, J.P., 1994, Nature, 370, 423

Misawa, T., Gandhi, P., Hida, A., Tamagawa, T., & Yamaguchi, T., 2009, ApJ, 700, 1988

Moutou, C., Sellgren, K., Verstraete, L., & Léger, A., 1999, A&A, 347, 949

Nuccitelli, D., Richter, M.J., & McCall, B.J., 2005, IAU Symp., 235, 236

Pascoli, G., & Polleux, A., 2000, A&A, 359, 799

Scott, A., Duley, W.W., & Pinho, G.P., 1997, ApJ, 489, L193

Sellgren, K., Uchida, K.I., & Werner, M.W., 2007, ApJ, 659, 1338

Smith, J.D.T., *et al.*, 2007a, ApJ, 656, 770

Smith, J.D.T., *et al.*, 2007b, PASP, 119, 1133

Snow, T.P., & Seab, C.G., 1989, A&A, 213, 291

Sogoshi, N., Kato, Y., Wakabayashi, T., *et al.*, 2000, J. Phys. Chem. A., 104, 3733

Somerville, W.B., & Bellis, J.G., 1989, MNRAS, 240, 41P

Tielens, A.G.G.M., 2008, ARA&A, 46, 289

Werner, M.W., *et al.*, 2004, ApJS, 154, 1

Werner, M.W., *et al.*, 2004, ApJS, 154, 309

Yagi, H., *et al.*, 2009, Carbon, 47, 1152

Yasumatsu, H., Kondow, T., Kitagawa, H., Tabayashi, K., & Shobatake, K., 1996, J. Chem. Phys., 104, 899